

Analysis of a Class of Symmetric Equilibrium Configurations for a Territorial Model

Michael Busch* and Jeff Moehlis

Department of Mechanical Engineering, University of California, Santa Barbara, CA 93106, USA.

Received 15 September 2009; Accepted (in revised version) 6 January 2010

Available online 8 March 2010

Abstract. Motivated by an animal territoriality model, we consider a centroidal Voronoi tessellation algorithm from a dynamical systems perspective. In doing so, we discuss the stability of an aligned equilibrium configuration for a rectangular domain that exhibits interesting symmetry properties. We also demonstrate the procedure for performing a center manifold reduction on the system to extract a set of coordinates which capture the long term dynamics when the system is close to a bifurcation. Bifurcations of the system restricted to the center manifold are then classified and compared to numerical results. Although we analyze a specific set-up, these methods can in principle be applied to any bifurcation point of any equilibrium for any domain.

AMS subject classifications: 37N25, 37G10

Key words: Territorial behavior, Voronoi tessellations, bifurcation, center manifold reduction.

1. Introduction

A *territory* is a geographical area that an individual animal consistently defends against other individuals from its own species, typically in an attempt to maximize its reproductive opportunities and/or to secure food resources for itself and its young [11]. Territoriality is common across nearly all major groups of organisms on the planet. While higher animals like vertebrates exhibit the most obvious territorial boundaries, lower animals like invertebrates, plants, fungi and possibly even bacteria are known to aggressively defend space through behaviors and chemicals.

The recent paper [10] studied equilibrium configurations for a model for territorial behavior based on Voronoi tessellations, which captures interactions between agents in a simple way [9]; also see [3, 6, 7]. For this model, at a given time and for each agent, one calculates the set of points in the domain of interest which are closer to that agent than to any other. Such a partition of the domain is called a Voronoi tessellation, and the set of

*Corresponding author. *Email addresses:* mbusch@engineering.ucsb.edu (M. Busch), moehlis@engineering.ucsb.edu (J. Moehlis)

such points for each agent is called the agent's Voronoi cell. The agents then move toward the centroid of their Voronoi cell, continuing such adjustment until an equilibrium state is reached. An agent's Voronoi cell at such an equilibrium is considered to be its territory. We note that these equilibria are centroidal Voronoi tessellations, that is, Voronoi tessellations for which the generators of the Voronoi cells are the centroids of the cells defined using a constant density function [3]. This model captures the tendency of each agent to occupy territory so that it is as far from others as possible, and the notion that aggression of an agent decreases monotonically with distance from the center of its territory. It ignores environmental influences and heterogeneity in the individuals' characteristics or behavior. We remark that related models based on Voronoi tessellations have become popular in the robotics literature, e.g. [2, 5, 8], where the motivation might be the performance of spatially distributed sensing tasks such as surveillance or search and rescue.

This model was considered in detail in [10] for rectangular domains, with the boundaries of the domain forming boundaries of the Voronoi cells as appropriate. The analysis included a numerical bifurcation analysis for which the ratio L of the length of the shorter side to the length of the longer side of the rectangle was treated as a bifurcation parameter. This showed numerically how equilibrium configurations are related to each other through bifurcations, and identified ranges of L for which coexisting stable equilibrium configurations occur.

For a rectangular domain with any L , there are equilibrium configurations in which all agents are aligned. As shown in [10], such configurations can be stable or unstable depending on the number of agents and the value of L , and they can undergo bifurcations as L is varied. In this paper, we consider the stability and bifurcation behavior of these configurations analytically. In particular, in Sections 2 and 3 we respectively specify the territorial model and the aligned equilibrium configurations more precisely. In Section 4 we calculate the eigenvalues and eigenvectors associated with the linearization about such equilibrium configurations, and in Section 5 we identify parameter values at which bifurcations occur. In Section 6 we perform a center manifold reduction for small numbers of agents, which captures the asymptotic dynamics of the system near the bifurcation. The analysis of the dynamics reduced to the center manifold allows a classification of the bifurcation which occurs for the system. For a system with two agents, the results from the center manifold analysis are shown to be consistent with results from an alternative treatment given in the Appendix. Finally, Section 8 gives concluding remarks.

2. Model description

The model studied in [10] considers N agents in a two-dimensional rectangular domain D with sides of length 1 and L . The location of the i^{th} agent at time step n is $\mathbf{x}_i^{(n)}$. The Voronoi cell [3] for the i^{th} agent at time step n is defined as

$$V_i^{(n)} = \left\{ \mathbf{x} \in D \mid |\mathbf{x} - \mathbf{x}_i^{(n)}| < |\mathbf{x} - \mathbf{x}_j^{(n)}| \text{ for } j = 1, \dots, N, j \neq i \right\},$$

with centroid

$$c_i^{(n)} = \frac{1}{|V_i^{(n)}|} \int_{V_i^{(n)}} \mathbf{x} d\mathbf{x}, \tag{2.1}$$

where $|V_i^{(n)}|$ is the area of Voronoi cell $V_i^{(n)}$. As proposed in [9] for describing the dynamics of the animal territoriality problem based on centroidal Voronoi tessellations, we too shall take each agent's location at time step $n + 1$ as

$$\mathbf{x}_i^{(n+1)} = \mathbf{x}_i^{(n)} + \left(c_i^{(n)} - \mathbf{x}_i^{(n)} \right) / M, \quad i = 1, \dots, N, \tag{2.2}$$

where M is a constant greater than or equal to 1. It can be shown that (2.2) can be reformulated as a gradient descent method, as discussed in [3]. An equilibrium solution of (2.2) has the property that

$$\mathbf{x}_i^{(n+1)} = \mathbf{x}_i^{(n)}, \quad i = 1, \dots, N.$$

3. The aligned equilibrium configuration

For a system of N agents in a two-dimensional x - y plane centered at the origin, letting $\mathbf{x}_i = (x_i, y_i)$ and $\mathbf{c}_i = (c_{ix}, c_{iy})$ allows one to construct the governing equations for the positions of each agent in terms of their x and y components:

$$x_i^{(n+1)} = x_i^{(n)} + \left(c_{ix}^{(n)} - x_i^{(n)} \right) / M \equiv \hat{f}_{ix} \left(x_1^{(n)}, \dots, x_N^{(n)}, y_1^{(n)}, \dots, y_N^{(n)} \right), \tag{3.1}$$

$$y_i^{(n+1)} = y_i^{(n)} + \left(c_{iy}^{(n)} - y_i^{(n)} \right) / M \equiv \hat{f}_{iy} \left(x_1^{(n)}, \dots, x_N^{(n)}, y_1^{(n)}, \dots, y_N^{(n)} \right), \tag{3.2}$$

for $i = 1, \dots, N$. We choose the domain to be the set

$$D = \left\{ (x, y) \mid -\frac{1}{2} \leq x \leq \frac{1}{2}, -\frac{L}{2} \leq y \leq \frac{L}{2} \right\},$$

and will consider the equilibrium configuration where the agents are aligned along the y -axis, so that the equilibrium positions for the i^{th} agent is $\mathbf{x}_{eq,i} = (x_{eq,i}, y_{eq,i})$, where

$$\begin{aligned} x_{eq,i} &= 0, \\ y_{eq,i} &= \frac{L}{2} \left(1 - \frac{(2i-1)}{N} \right), \quad i = 1, \dots, N. \end{aligned} \tag{3.3}$$

Here we have imposed an order on the agents for reference, where the index values are assigned sequentially from 1 to N as the agents are counted from top to bottom as show in Fig. 1.

This aligned equilibrium configuration is interesting for several reasons. Not only does it exist for all values of L , M , and N , but it does so because of its interesting symmetry properties. For instance, at this equilibrium we emphasize that each agent's Voronoi cell is congruent and symmetric about the axis of alignment.

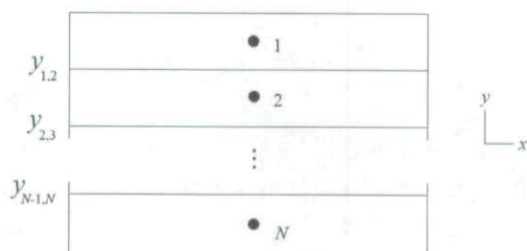


Figure 1: An illustration of agent ordering near the aligned equilibrium.

With knowledge of the equilibrium and the rules that govern the shape of the cell, analytic expressions can be formed for the cell properties of each agent when it is close to the aligned equilibrium. Suppose one were to consider any two adjacent agents $\mathbf{a}_i = (x_i, y_i)$ and $\mathbf{a}_j = (x_j, y_j)$ nearly aligned vertically on the x - y plane. Requiring \mathbf{a}_i and \mathbf{a}_j to be adjacent asserts that \mathbf{a}_i and \mathbf{a}_j have consecutive indices so that $j = i + 1$ or $j = i - 1$ according to the spatial orientation specified by (3.3) and Fig. 1. The set of points that are equidistant to \mathbf{a}_i and \mathbf{a}_j are located on a line, $y_{i,j}$, that intersects the midpoint of, and is perpendicular to, the segment $\overline{\mathbf{a}_i \mathbf{a}_j}$. The line $y_{i,j}$ divides the sets of points that are closest to \mathbf{a}_i and \mathbf{a}_j respectively, and is given in terms of y as a function of x ,

$$y_{i,j}(x) = \frac{x_j - x_i}{y_i - y_j} \left(x - \frac{1}{2} (x_i + x_j) \right) + \frac{1}{2} (y_i + y_j), \quad -\frac{1}{2} \leq x \leq \frac{1}{2}. \quad (3.4)$$

For reference, the $y_{1,2}$, $y_{2,3}$, and $y_{N-1,N}$ lines are depicted in Figure 1 and are labeled to the left of their respective lines. We remark that (3.4) relies on the agents being close enough to equilibrium so that no $y_{i,j}$ lines intersect.

With the bounds of the parameterized rectangular domain at $x = \pm \frac{1}{2}$ and $y = \pm \frac{L}{2}$, enough is known to construct analytic expressions for the volumes

$$V_i^{(n)} = \int_{-\frac{1}{2}}^{\frac{1}{2}} \int_{y_{i,i+1}(x)}^{y_{i-1,i}(x)} dy dx, \quad i = 1, \dots, N, \quad (3.5)$$

and component-wise expressions for the centroids of each cell

$$c_{y,i}^{(n)} = \frac{1}{|V_i^{(n)}|} \int_{-\frac{1}{2}}^{\frac{1}{2}} \int_{y_{i,i+1}(x)}^{y_{i-1,i}(x)} y dy dx, \quad (3.6)$$

$$c_{x,i}^{(n)} = \frac{1}{|V_i^{(n)}|} \int_{-\frac{1}{2}}^{\frac{1}{2}} \int_{y_{i,i+1}(x)}^{y_{i-1,i}(x)} x dy dx, \quad i = 1, \dots, N. \quad (3.7)$$

In (3.5)-(3.7) it is understood that $y_{0,1} = L/2$ and $y_{N,N+1} = -L/2$.

In anticipation of performing a Taylor series expansion of (3.1) and (3.2), the equilibrium shall be translated to the origin to simplify the calculation. In the case of the vertically

aligned equilibrium configuration, only the coordinates corresponding with the y -direction need to be translated. We let

$$z_i^{(n)} = y_i^{(n)} - y_{eq,i}, \tag{3.8}$$

$$z_i^{(n+1)} = y_i^{(n+1)} - y_{eq,i}. \tag{3.9}$$

In the new coordinates we have

$$\begin{pmatrix} x_i^{(n+1)} \\ z_i^{(n+1)} \end{pmatrix} = \begin{pmatrix} f_{ix} \left(x_1^{(n)}, \dots, x_N^{(n)}, z_1^{(n)}, \dots, z_N^{(n)} \right) \\ f_{iz} \left(x_1^{(n)}, \dots, x_N^{(n)}, z_1^{(n)}, \dots, z_N^{(n)} \right) - y_{eq,i} \end{pmatrix}, \quad i = 1, \dots, N, \tag{3.10}$$

where f_{ix} is the function obtained by rewriting \widehat{f}_{ix} as a function of the x_i and z_i coordinates from the substitution of (3.8)-(3.9), and similar for obtaining f_{iz} from \widehat{f}_{iz} . In these new coordinates, the Voronoi cells are symmetric about the origin of each agent's respective x_i and z_i coordinates.

We remark that (3.10) consists of expressions (3.4)-(3.7) and (3.3), which are all in terms of the parameterized aspect ratio L , total number of agents N , and agent indices $i - 1$, i , and $i + 1$ for each x and z component. To understand the dynamics of the system near the equilibrium $(x_i, z_i) = (0, 0)$, one calculates a Taylor series expansion of (3.10) about the equilibrium and considers only the linear terms to get

$$\begin{pmatrix} x_i^{(n+1)} \\ z_i^{(n+1)} \end{pmatrix} \approx \begin{pmatrix} -\frac{N^2}{12ML^2} x_{i-1}^{(n)} + \left(1 - \frac{1}{M} + \frac{N^2}{6ML^2}\right) x_i^{(n)} - \frac{N^2}{12ML^2} x_{i+1}^{(n)} \\ \frac{1}{4M} z_{i-1}^{(n)} + \left(1 - \frac{1}{2M}\right) z_i^{(n)} + \frac{1}{4M} z_{i+1}^{(n)} \end{pmatrix}, \tag{3.11}$$

$i = 2, \dots, N - 1.$

Eq. (3.11) only considers agents a_i for which $i = 2, \dots, N - 1$ because agents a_1 and a_N are adjacent to the domain boundary at $y = L/2$ and $y = -L/2$ where the coordinates $(x_{i-1}, z_{i-1}) = (x_0, z_0)$ and $(x_{i+1}, z_{i+1}) = (x_{N+1}, z_{N+1})$ do not exist. We evaluate (3.4)-(3.7) for $y_{0,1} = L/2$ and $y_{N,N+1} = -L/2$, and calculate the Taylor series of (3.10) to first order about the equilibrium for $i = 1, N$ to get,

$$\begin{pmatrix} x_1^{(n+1)} \\ z_1^{(n+1)} \end{pmatrix} = \begin{pmatrix} \left(1 - \frac{1}{M} + \frac{N^2}{6ML^2}\right) x_1^{(n)} - \frac{N^2}{12ML^2} x_2^{(n)} \\ \left(1 - \frac{3}{4M}\right) z_1^{(n)} + \frac{1}{4M} z_2^{(n)} \end{pmatrix}, \tag{3.12}$$

and

$$\begin{pmatrix} x_N^{(n+1)} \\ z_N^{(n+1)} \end{pmatrix} = \begin{pmatrix} -\frac{N^2}{12ML^2} x_{N-1}^{(n)} + \left(1 - \frac{1}{M} + \frac{N^2}{6ML^2}\right) x_N^{(n)} \\ \frac{1}{4M} z_{N-1}^{(n)} + \left(1 - \frac{3}{4M}\right) z_N^{(n)} \end{pmatrix}, \tag{3.13}$$

where the higher order terms are truncated.

Because the x and y directions are decoupled when linearizing about the equilibrium, so are the x and z directions. The coordinates corresponding with the x -components can

be grouped separate from the z -components to produce a block-diagonal Jacobian matrix. It follows from the results of (3.11)-(3.13) that the Jacobian matrix evaluated about the origin for a system of any number of agents becomes

$$J = \begin{pmatrix} \frac{\partial f_{1x}}{\partial x_1} & \frac{\partial f_{1x}}{\partial x_2} & \dots & \frac{\partial f_{1x}}{\partial x_N} & \frac{\partial f_{1x}}{\partial z_1} & \frac{\partial f_{1x}}{\partial z_2} & \dots & \frac{\partial f_{1x}}{\partial z_N} \\ \frac{\partial f_{2x}}{\partial x_1} & \frac{\partial f_{2x}}{\partial x_2} & \dots & \frac{\partial f_{2x}}{\partial x_N} & \frac{\partial f_{2x}}{\partial z_1} & \frac{\partial f_{2x}}{\partial z_2} & \dots & \frac{\partial f_{2x}}{\partial z_N} \\ \vdots & \vdots & \ddots & \vdots & \vdots & \vdots & \ddots & \vdots \\ \frac{\partial f_{Nx}}{\partial x_1} & \frac{\partial f_{Nx}}{\partial x_2} & \dots & \frac{\partial f_{Nx}}{\partial x_N} & \frac{\partial f_{Nx}}{\partial z_1} & \frac{\partial f_{Nx}}{\partial z_2} & \dots & \frac{\partial f_{Nx}}{\partial z_N} \\ \hline \frac{\partial f_{1z}}{\partial x_1} & \frac{\partial f_{1z}}{\partial x_2} & \dots & \frac{\partial f_{1z}}{\partial x_N} & \frac{\partial f_{1z}}{\partial z_1} & \frac{\partial f_{1z}}{\partial z_2} & \dots & \frac{\partial f_{1z}}{\partial z_N} \\ \frac{\partial f_{2z}}{\partial x_1} & \frac{\partial f_{2z}}{\partial x_2} & \dots & \frac{\partial f_{2z}}{\partial x_N} & \frac{\partial f_{2z}}{\partial z_1} & \frac{\partial f_{2z}}{\partial z_2} & \dots & \frac{\partial f_{2z}}{\partial z_N} \\ \vdots & \vdots & \ddots & \vdots & \vdots & \vdots & \ddots & \vdots \\ \frac{\partial f_{Nz}}{\partial x_1} & \frac{\partial f_{Nz}}{\partial x_2} & \dots & \frac{\partial f_{Nz}}{\partial x_N} & \frac{\partial f_{Nz}}{\partial z_1} & \frac{\partial f_{Nz}}{\partial z_2} & \dots & \frac{\partial f_{Nz}}{\partial z_N} \end{pmatrix}$$

$$\equiv \left(\begin{array}{c|c} J_{x,N} & 0 \\ \hline 0 & J_{z,N} \end{array} \right), \tag{3.14}$$

where the $J_{x,N}$ and $J_{z,N}$ blocks have the symmetric tri-diagonal structure

$$J_{\cdot,N} = \begin{pmatrix} b+c & a & 0 & 0 & \dots & 0 & 0 \\ a & b & a & 0 & \dots & 0 & 0 \\ 0 & a & b & a & \dots & 0 & 0 \\ \vdots & \vdots & \vdots & \vdots & \ddots & \vdots & \vdots \\ 0 & 0 & 0 & 0 & \dots & a & b+c \end{pmatrix}_{N \times N}, \tag{3.15}$$

with $c = a$ for the $J_{x,N}$ block and $c = -a$ for the $J_{z,N}$ block. In particular, the a and b elements of $J_{x,N}$ are $-N^2/(12ML^2)$ and $1 - 1/M + N^2/(6ML^2)$, while the a and b elements of $J_{z,N}$ are $1/(4M)$ and $1 - 1/(2M)$, respectively.

For example, the $J_{x,N}$ and $J_{y,N}$ blocks for the $N = 2, 3$ cases are

$$J_{x,2} = \frac{1}{M} \begin{pmatrix} M + \frac{1}{3L^2} - 1 & -\frac{1}{3L^2} \\ -\frac{1}{3L^2} & M + \frac{1}{3L^2} - 1 \end{pmatrix}, \quad J_{y,2} = \begin{pmatrix} 1 - \frac{3}{4M} & \frac{1}{4M} \\ \frac{1}{4M} & 1 - \frac{3}{4M} \end{pmatrix}, \tag{3.16}$$

$$J_{x,3} = \frac{1}{M} \begin{pmatrix} M + \frac{3}{4L^2} - 1 & -\frac{3}{4L^2} & 0 \\ -\frac{3}{4L^2} & M + \frac{2L^2}{3} - 1 & -\frac{3}{4L^2} \\ 0 & -\frac{3}{4L^2} & M + \frac{3}{4L^2} - 1 \end{pmatrix}, \tag{3.17}$$

$$J_{y,3} = \begin{pmatrix} 1 - \frac{3}{4M} & \frac{1}{4M} & 0 \\ \frac{1}{4M} & 1 - \frac{1}{2M} & \frac{1}{4M} \\ 0 & \frac{1}{4M} & 1 - \frac{3}{4M} \end{pmatrix}. \tag{3.18}$$

4. Eigenvalues and eigenvectors

For matrices of the structure (3.15), general expressions for the eigenvalues and eigenvectors have been developed by Yueh [12]. When adapted to the case of symmetric tridiagonal matrices, the general expression for the eigenvalues becomes

$$\lambda_k = b + 2a \cos \theta_k, \quad k = 1, 2, \dots, N, \tag{4.1}$$

and the general expression for the eigenvectors $u^{(k)} = (u_1^{(k)}, \dots, u_N^{(k)})$ is

$$u_j^{(k)} = \frac{1}{\sin \theta_k} \left(\sin(j\theta_k) - \frac{c}{|a|} \sin[(j-1)\theta_k] \right),$$

$$\text{for } j = \{1, 2, \dots, N\}, \text{ and } k = \{1, 2, \dots, N\}. \tag{4.2}$$

For the case where $c = a$,

$$u_j^{(k)} = 1, \quad \text{for } j = \{1, 2, \dots, N\}, \text{ and } k = 1, \tag{4.3}$$

and similarly when $c = -a$,

$$u_j^{(k)} = (-1)^{(j-1)}, \quad \text{for } j = \{1, 2, \dots, N\}, \text{ and } k = N. \tag{4.4}$$

Here, k is the vector index, j is the vector element index, and θ_k is $(k-1)\pi/N$ and $k\pi/N$ for the $c = a$ and $c = -a$ cases, respectively.

Since the a and b elements of the $J_{x,N}$ and $J_{y,N}$ blocks have been found for an arbitrary number of agents, solving for the eigenvalues and eigenvectors is simple. In particular, the eigenvalues contributed by the $J_{y,N}$ block will always have a modulus less than 1, as follows:

Proposition 4.1. *The eigenvalues of the $J_{y,N}$ block always lie within the unit circle.*

Proof. Substitute $a = \frac{1}{4M}$ and $b = 1 - \frac{1}{2M}$ into (4.1) to obtain

$$\lambda_k = 1 + \frac{1}{2M} (-1 + \cos \theta_k), \quad k = 1, \dots, N.$$

For finite values of M and $\theta_k = k\pi/N$ for the y -block, imposing the constraints $M \geq 1$ and $0 < \theta_k \leq \pi$ allow bounds to be placed on λ_k for $k = 1, \dots, N$

$$0 \leq \lambda_k < 1.$$

Therefore, the eigenvalues of the $J_{y,N}$ block strictly lie within the unit circle. □

Similarly, the expression for the $J_{x,N}$ block eigenvalues are found by substituting the a and b terms into (4.1) to get

$$\lambda_k = 1 + \frac{1}{M} \left(-1 + \frac{N^2}{6L^2} \left(1 - \cos \frac{(k-1)\pi}{N} \right) \right), \quad k = 1, \dots, N. \tag{4.5}$$

The significance of this eigenvalue analysis is in the conclusion that the $J_{y,N}$ block will always have stable eigenvalues, whereas the modulus of the $J_{x,N}$ eigenvalues depends on L . Thus, one only needs to restrict attention to $J_{x,N}$ to find the bifurcation points and determine the stability of the system in this aligned configuration.

5. Bifurcation points

A "bifurcation" is a qualitative change in the dynamics of a system as a parameter is varied [4]. Moreover, a "bifurcation point" is defined as the parameter value where a bifurcation occurs. Specifically, the qualitative change of interest in this paper will be the loss of asymptotic stability of the aligned equilibrium configuration.

To define asymptotic stability, suppose an equilibrium configuration described by the set of points \mathbf{x}_{EQ} exists for the system defined by (3.1) and (3.2). Here, \mathbf{x}_{EQ} is asymptotically stable if and only if there exists a constant $0 < b < 1$ such that

$$\|\mathbf{x}^{(n+1)} - \mathbf{x}_{EQ}\| < b\|\mathbf{x}^{(n)} - \mathbf{x}_{EQ}\|.$$

Otherwise, \mathbf{x}_{EQ} is said to be unstable. For an equilibrium to be asymptotically stable, all of the eigenvalues of the Jacobian evaluated at the equilibrium must lie within the unit circle.

We look for bifurcations by examining the $J_{x,N}$ block eigenvalues parameterized by L , of which there are $N - 1$ because (4.5) shows that the $k = 1$ eigenvalue will always be $1 - 1/M$. The locations of these bifurcations in terms of the parameter L for an arbitrary number of agents, N , readily comes from the expression (4.5) for the eigenvalues, λ_k . Because the Jacobian is symmetric, the eigenvalues must necessarily be real. Therefore, one can deduce that bifurcations may occur at real parameter values $L = L_{b,k}$ for which $\lambda_k = 1$, namely

$$L_{b,k} = \sqrt{\frac{N^2}{6} \left(1 - \cos \frac{(k-1)\pi}{N} \right)}, \quad k = 2, \dots, N.$$

The vertically aligned equilibrium configuration is asymptotically stable if $1 > \lambda_k$ for $k = N$, and from (4.5), $\lambda_N \geq \lambda_{N-1} \geq \dots \geq \lambda_1$. This indicates that the bifurcation value

$$L_b = L_{b,k} = \sqrt{\frac{N^2}{6} \left(1 - \cos \frac{(N-1)\pi}{N} \right)} \quad (5.1)$$

is of particular interest because it is where the vertically aligned equilibrium configuration changes stability. For large N , (5.1) can be approximated by the simple expression $L_b \approx N/\sqrt{3}$. The L_b parameter values predicted by (5.1) are compared to numerical data in Fig. 2, where the numerical data was collected by detecting the point where the first eigenvalue crosses the unit circle for the aligned equilibrium branch of solutions.

For $L > L_b$ the aligned configuration is asymptotically stable. We remark that there might be other coexisting stable configurations for such L ; if this is the case, each configuration will have its own basin of attraction. As in [10], by considering uniformly distributed random initial conditions we can obtain a statistical characterization of the sizes of the basins of attraction for the different coexisting stable equilibrium configurations. This analysis shows that the size of the basin of attraction of the aligned equilibrium configuration grows from zero as we increase L beyond the bifurcation point. From the numerical results in [10], when L becomes sufficiently large, the aligned equilibrium is the only attractor.

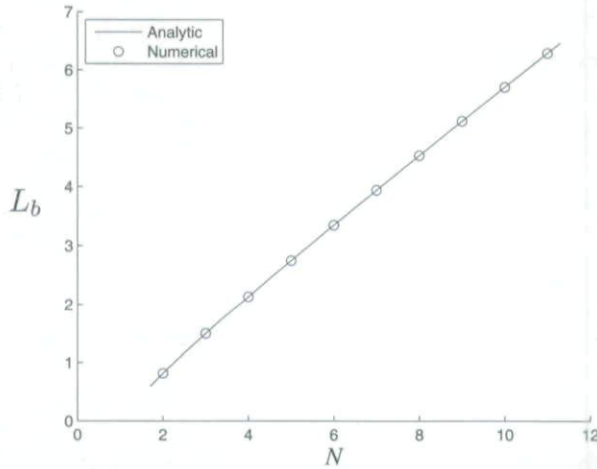


Figure 2: Comparison of the analytic expression (5.1) to the numerical results for bifurcation points of the aligned equilibrium configuration.

6. Augmented center manifold reduction

6.1. Center manifold construction and properties

For a system *at* a bifurcation point, a center manifold reduction can be applied to capture the system’s asymptotic dynamics. To capture the dynamics *near* a bifurcation point, one can treat the bifurcation parameter as a state variable with trivial dynamics: it remains constant. In doing so, the bifurcation parameter may be used in the reduction to allow further assessment of the bifurcation; when a parameter is treated like this, the reduction is called an augmented center manifold reduction.

The center manifold existence theorem proven by Carr [1] considers systems of the form

$$\begin{pmatrix} w^{(n+1)} \\ v^{(n+1)} \\ u^{(n+1)} \end{pmatrix} = \begin{pmatrix} Aw^{(n)} + f(w^{(n)}, v^{(n)}, u^{(n)}) \\ Bv^{(n)} + g(w^{(n)}, v^{(n)}, u^{(n)}) \\ Cu^{(n)} + h(w^{(n)}, v^{(n)}, u^{(n)}) \end{pmatrix},$$

$$(w^{(n)}, v^{(n)}, u^{(n)}) \in R^{n_c} \times R^{n_s} \times R^{n_u}, \tag{6.1}$$

where

$$\begin{aligned} f(0, 0, 0) &= 0, & Df(0, 0, 0) &= 0, \\ g(0, 0, 0) &= 0, & Dg(0, 0, 0) &= 0, \\ h(0, 0, 0) &= 0, & Dh(0, 0, 0) &= 0, \end{aligned}$$

and the functions *f*, *g* and *h* are at least twice differentiable in some neighborhood about the origin. Furthermore, *A* is an $n_c \times n_c$ matrix having eigenvalues on the unit circle, *B* is

an $n_s \times n_s$ matrix having eigenvalues with modulus less than 1, and C is an $n_u \times n_u$ matrix having eigenvalues with modulus greater than 1.

The existence theorem for center manifolds states that for systems of the form above, there exists an invariant center manifold, W^c , that is at least twice differentiable and can be locally represented as

$$W^c(0) = \left\{ (w, v, u) \in R^{n_c} \times R^{n_s} \times R^{n_u} \mid v = \kappa_1(w), u = \kappa_2(w), \right. \\ \left. |w| < \delta, \kappa_i(0) = 0, D\kappa_i(0) = 0, i = 1, 2 \right\}, \quad (6.2)$$

for w sufficiently small. The mapping restricted to the center manifold is

$$w^{(n+1)} = Aw^{(n)} + f(w^{(n)}, \kappa_1(w^{(n)}), \kappa_2(w^{(n)})), \quad w \in R^{n_c}. \quad (6.3)$$

It follows that when a bifurcation parameter is included as a state on the center manifold, all bifurcating solutions involving that bifurcation parameter will also be contained on the center manifold, particularly when the center manifold is found locally near a bifurcation point. Eventually, we will construct a center manifold that has the parameter value as one of the coordinates such that L will be treated as though it depends on the iteration step n , $L^{(n)}$. We remark that L is still a constant, i.e., $L^{(n+1)} = L^{(n)}$.

Similar to (3.8) and (3.9), the bifurcation point can be translated to the origin

$$\mu^{(n)} = L^{(n)} - L_b, \quad (6.4a)$$

$$\mu^{(n+1)} = \mu^{(n)}. \quad (6.4b)$$

The augmented system of equations for the vertically aligned equilibrium configuration becomes

$$\begin{pmatrix} \mu^{(n+1)} \\ x_i^{(n+1)} \\ z_i^{(n+1)} \end{pmatrix} = \begin{pmatrix} \mu^{(n)} \\ f_{ix} \left(x_1^{(n)}, \dots, x_N^{(n)}, z_1^{(n)}, \dots, z_N^{(n)}; \mu \right) \\ f_{iz} \left(x_1^{(n)}, \dots, x_N^{(n)}, z_1^{(n)}, \dots, z_N^{(n)}; \mu \right) - y_{eq,i} \end{pmatrix}, \quad (6.5)$$

for $i = 1, \dots, N$. It may be unclear which combinations of coordinates correspond with eigenvalues on the unit circle, and those which do not. To distinguish the center, stable, and unstable coordinates, (6.5) is linearized about the origin and the Jacobian is diagonalized by a similarity transformation

$$\phi^{(n)} = P^{-1} \mathbf{x}^{(n)}, \quad (6.6a)$$

$$\begin{aligned} \phi^{(n+1)} &= P^{-1} \mathbf{x}^{(n+1)} \\ &= P^{-1} J P \phi^{(n)}, \end{aligned} \quad (6.6b)$$

where P is a matrix whose columns are the eigenvectors of the Jacobian of (6.5), and $P^{-1}JP$ is a diagonal matrix with the diagonal elements being the eigenvalues of J . The new coordinates ϕ_i consist of the center, stable, and unstable sets of coordinates as described

in (6.1). The center manifold is then constructed by representing the stable and unstable coordinates of the decoupled system in terms of the center coordinates by means of a Taylor series approximation about the bifurcation point.

Next, the coefficients in the Taylor series are found by requiring the center manifold to be invariant under iterations of the map, i.e., $v^{(n+1)} = \kappa_1(w^{(n+1)})$ and $u^{(n+1)} = \kappa_2(w^{(n+1)})$, so

$$0 = B\kappa_1(w^{(n)}) + g(w^{(n)}, \kappa_1(w^{(n)}), \kappa_2(w^{(n)})) - \kappa_1(Aw^{(n)} + f(w^{(n)}, \kappa_1(w^{(n)}), \kappa_2(w^{(n)}))), \quad (6.7a)$$

$$0 = C\kappa_2(w^{(n)}) + h(w^{(n)}, \kappa_1(w^{(n)}), \kappa_2(w^{(n)})) - \kappa_2(Aw^{(n)} + f(w^{(n)}, \kappa_1(w^{(n)}), \kappa_2(w^{(n)}))). \quad (6.7b)$$

When the Taylor series are substituted for v and u in (6.1), the dynamics on the center manifold are expressed in terms of the center coordinates, c.f. (6.2). We emphasize that the augmented center manifold procedure produces the bifurcation parameter as one of the center coordinates.

This method can be used to construct the center manifold when there are both asymptotically stable and unstable directions. The center manifold becomes more significant, however, if no unstable directions exist, which is the situation when one only considers the local dynamics about the bifurcation point corresponding with the $k = N$ eigenvalue of the $J_{x,N}$ block as shown in expression (5.1). Then the stability theorem proven by Carr [1] for center manifolds asserts that if the zero solution of (6.3) is stable (asymptotically stable) (unstable), then the zero solution of (6.1) is stable (asymptotically stable) (unstable). In other words, if none of the coordinates correspond to eigenvalues with modulus greater than 1, then the dynamics on the center manifold capture the asymptotic dynamics of the full system.

6.2. Example: center manifold reduction for $N=2$

The two agent system can be used to demonstrate the augmented center manifold reduction procedure for which $L_b = \sqrt{2/3}$. Here we begin with the system of equations,

$$\begin{aligned} \mu^{(n+1)} &= \mu, \\ x_1^{(n+1)} &= f_{1x}(\mu, x_1, x_2, z_1, z_2), \\ x_2^{(n+1)} &= f_{2x}(\mu, x_1, x_2, z_1, z_2), \\ z_1^{(n+1)} &= f_{1z}(\mu, x_1, x_2, z_1, z_2) + \left(\mu + \sqrt{2/3}\right)/4, \\ z_2^{(n+1)} &= f_{2z}(\mu, x_1, x_2, z_1, z_2) - \left(\mu + \sqrt{2/3}\right)/4. \end{aligned}$$

When linearized about the origin, the resulting linear system has the eigenvalues and corresponding eigenvectors

$$\begin{aligned} \text{Eigenvalues:} & \quad 1, 1, 1 - \frac{1}{M}, 1 - \frac{1}{M}, 1 - \frac{1}{2M}, \\ \text{Eigenvectors:} & \quad \begin{pmatrix} 1 \\ 0 \\ 0 \\ 0 \\ 0 \end{pmatrix}, \begin{pmatrix} 0 \\ 1 \\ -1 \\ 0 \\ 0 \end{pmatrix}, \begin{pmatrix} 0 \\ 1 \\ 1 \\ 0 \\ 0 \end{pmatrix}, \begin{pmatrix} 0 \\ 0 \\ 0 \\ 1 \\ -1 \end{pmatrix}, \begin{pmatrix} 0 \\ 0 \\ 0 \\ 1 \\ 1 \end{pmatrix}. \end{aligned}$$

Let P be a matrix for which the columns are these eigenvectors. The change of coordinates (6.6a) produces $\phi = (\mu, \chi, S_1, S_2, S_3)^T$

$$\begin{aligned} \mu &= \mu \quad (\text{unchanged}), & \chi &= (x_1 - x_2) / 2, & S_1 &= (x_1 + x_2) / 2, \\ S_2 &= (z_1 - z_2) / 2, & S_3 &= (z_1 + z_2) / 2. \end{aligned}$$

From the linearized state equations in the new coordinates, the variables χ and μ correspond with eigenvalues that lie on the unit circle, and thus compose the center manifold according to (6.2). The other variables have eigenvalues that lie inside the unit circle, and are approximated by a power series in terms of the center coordinates

$$S_1(\chi, \mu) = \alpha_1\mu^2 + \alpha_2\mu\chi + \alpha_3\chi^2 + \alpha_4\mu^3 + \alpha_5\mu^2\chi + \alpha_6\mu\chi^2 + \alpha_7\chi^3 + \mathcal{O}((\chi + \mu)^4), \tag{6.8}$$

$$S_2(\chi, \mu) = \beta_1\mu^2 + \beta_2\mu\chi + \beta_3\chi^2 + \beta_4\mu^3 + \beta_5\mu^2\chi + \beta_6\mu\chi^2 + \beta_7\chi^3 + \mathcal{O}((\chi + \mu)^4), \tag{6.9}$$

$$S_3(\chi, \mu) = \gamma_1\mu^2 + \gamma_2\mu\chi + \gamma_3\chi^2 + \gamma_4\mu^3 + \gamma_5\mu^2\chi + \gamma_6\mu\chi^2 + \gamma_7\chi^3 + \mathcal{O}((\chi + \mu)^4), \tag{6.10}$$

where the α , β , and γ variables are the constants to be solved for. Using Mathematica to solve (6.7a) and (6.7b) with these power series, produces

$$S_1 = 0, \quad S_2 = \sqrt{6}\chi^2 + 3\mu\chi^2 + \mathcal{O}(\chi^4), \quad S_3 = 0,$$

and a center manifold of third order in (μ, χ) of the form

$$\mu^{(n+1)} = \mu^{(n)}, \tag{6.11}$$

$$\chi^{(n+1)} = \left(1 - \frac{\sqrt{6}\mu}{M}\right)\chi^{(n)} + \frac{12}{M}(\chi^{(n)})^3 + \mathcal{O}(\chi^4). \tag{6.12}$$

6.3. Center manifold reduction for $N=3,4$

A similar procedure can be used to obtain the mapping restricted to the center manifold for other N values. Here, we will find the augmented center manifolds for the $N = 3$ and

$N = 4$ cases. With the eigenvectors for the $N = 3$ and $N = 4$ Jacobian matrices are found from (4.2). By augmenting the eigenvectors to account for the $\mu^{(n+1)} = \mu^{(n)}$, we construct the P_N matrices

$$P_3 = \begin{pmatrix} 1 & 0 & 0 & 0 & 0 & 0 & 0 \\ 0 & 1 & 1 & 1 & 0 & 0 & 0 \\ 0 & -2 & 0 & 1 & 0 & 0 & 0 \\ 0 & 1 & -1 & 1 & 0 & 0 & 0 \\ 0 & 0 & 0 & 0 & 1 & 1 & 1 \\ 0 & 0 & 0 & 0 & -1 & 0 & 2 \\ 0 & 0 & 0 & 0 & 1 & -1 & 1 \end{pmatrix},$$

$$P_4 = \begin{pmatrix} 1 & 0 & 0 & 0 & 0 & 0 & 0 & 0 & 0 \\ 0 & 1 & 1 & 1 & 1 & 0 & 0 & 0 & 0 \\ 0 & -1-\sqrt{2} & -1 & -1+\sqrt{2} & 1 & 0 & 0 & 0 & 0 \\ 0 & 1+\sqrt{2} & -1 & 1-\sqrt{2} & 1 & 0 & 0 & 0 & 0 \\ 0 & -1 & 1 & -1 & 1 & 0 & 0 & 0 & 0 \\ 0 & 0 & 0 & 0 & 0 & 1 & 1 & 1 & 1 \\ 0 & 0 & 0 & 0 & 0 & -1 & 1-\sqrt{2} & 1 & 1+\sqrt{2} \\ 0 & 0 & 0 & 0 & 0 & 1 & 1-\sqrt{2} & -1 & 1+\sqrt{2} \\ 0 & 0 & 0 & 0 & 0 & -1 & 1 & -1 & 1 \end{pmatrix},$$

whose columns are the eigenvectors of the J_N matrix, and the inverse of each P_N matrix transforms the coordinates as $\phi_N = P_N^{-1}\mathbf{x} = (\mu, \chi, S_1, \dots, S_{2N-1})^T$. In both the P_3 and P_4 matrices, the first column is the eigenvector corresponding with the μ parameter, while the second column is the eigenvector that corresponds with the bifurcating eigenvalue. The remaining eigenvectors can be arranged in any order, especially since they are all stable, but for simplicity we chose to arrange the remaining eigenvectors in descending order of k for each block. By extending (6.8)-(6.10) to S_{2N-1} , we find the nonzero S_i expressions to be

$$N = 3: \quad \begin{aligned} S_2 &= -24\chi^3, \\ S_4 &= 6\chi^2 + 12\mu\chi^2, \end{aligned}$$

$$N = 4: \quad \begin{aligned} S_2 &= -84.4264\chi^3, \\ S_6 &= 10.9269\chi^2 + 29.8492\mu\chi^2, \end{aligned}$$

and obtain the center manifold equations

$$N = 3: \quad \chi^{(n+1)} = \left(1 - \frac{4\mu}{3M}\right)\chi^{(n)} + \frac{24}{M}(\chi^{(n)})^3 + \mathcal{O}(\chi^4), \tag{6.13}$$

$$N = 4: \quad \chi^{(n+1)} = \left(1 - \frac{0.937379\mu}{M}\right)\chi^{(n)} + \frac{40.9706}{M}(\chi^{(n)})^3 + \mathcal{O}(\chi^4). \tag{6.14}$$

7. Bifurcation classification

We first analyze the mapping restricted to the center manifold for $N = 2$. Since the parameter μ is constant under the dynamics of (6.11), it is only the χ coordinate that determines the dynamics on the center manifold. With essentially only one state equation to consider, the bifurcation becomes rather straightforward to analyze. Thus far, we know that a bifurcation occurs at the origin of (6.12), however it is as yet unknown if other solutions emerge or vanish at the bifurcation, or what their stability properties.

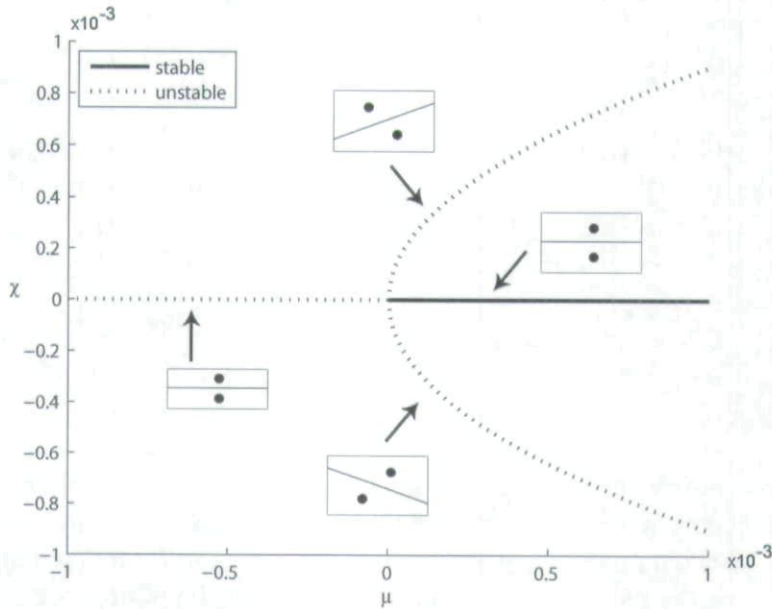


Figure 3: Graph of subcritical pitchfork bifurcation with equilibrium configurations for $N=2$.

Equilibria on the center manifold satisfy $\chi^{(n+1)} = \chi^{(n)}$, which using the cubic truncation of (6.12) becomes

$$\chi^{(n)} = \left(1 - \frac{\sqrt{6}\mu}{M}\right) \chi^{(n)} + \frac{12}{M} (\chi^{(n)})^3,$$

which reduces to

$$0 = \chi^{(n)} \left((\chi^{(n)})^2 - \frac{\sqrt{6}\mu}{12} \right). \tag{7.1}$$

Eq. (7.1) has equilibria located at $\chi^{(n)} = 0, \sqrt{\sqrt{6}\mu/12}$, and $-\sqrt{\sqrt{6}\mu/12}$. (These results are confirmed by the alternative, more physically intuitive analysis given in the Appendix). The first equilibrium exists for both positive and negative values of μ , while the others only exist for positive values of μ . Therefore, the bifurcation that occurs at the origin must be of the ‘pitchfork’ type, which gets its name from the graph of solutions of (7.1), as depicted in Fig. 3. This is not surprising since pitchfork bifurcations are expected to occur when

they involve equilibria which are invariant under a reflection symmetry. The nature of the pitchfork bifurcation can be understood by assessing the stability of the $\chi = 0$ equilibrium as a function of μ . The linearization of (6.12) about this equilibrium gives the Jacobian

$$D_\chi(0, \mu) = 1 - \frac{\sqrt{6}\mu}{M},$$

which has a modulus less than 1 for positive values of μ so that the equilibrium is asymptotically stable, and a modulus greater than 1 for negative values of μ so that the equilibrium is unstable. Since the additional equilibria are present for μ values for which the $x = 0$ equilibrium is stable, this bifurcation must be "subcritical". We note that the stability properties of the other equilibria can be determined by linearizing (6.12) about those equilibria. For example, the equilibrium at $(\chi, \mu) = (0.01, 0.0012/\sqrt{6})$ has the Jacobian

$$D_\chi \left(\frac{1}{100}, \frac{12}{10000\sqrt{6}} \right) = 1 + \frac{24}{10000M},$$

which is greater than 1, and thus indicates instability as predicted. We verify these results by comparing them with results from a numerical bifurcation analysis, as shown in Fig. 4(a).

Similarly, we classify bifurcations on the center manifold for $N = 3$ and $N = 4$. We begin by evaluating (6.13) and (6.14) at equilibrium, $\chi^{(n+1)} = \chi^{(n)}$, to get

$$N = 3: \quad 0 = \chi^{(n)} \left((\chi^{(n)})^2 - \frac{\mu}{18} \right), \tag{7.2}$$

$$N = 4: \quad 0 = \chi^{(n)} \left((\chi^{(n)})^2 - 0.0228793\mu \right). \tag{7.3}$$

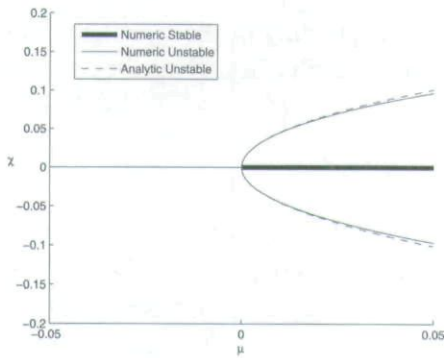
We note that solutions where $\chi^{(n)} \neq 0$ for (7.2) and (7.3) only exist for $\mu > 0$, which indicates the presence of pitchfork bifurcations in both cases. Likewise, the linearization of (6.13) and (6.14) about their respective $\chi^{(n)} = 0$ equilibria gives

$$N = 3: \quad D_\chi(0, \mu) = 1 - \frac{4\mu}{3M}, \tag{7.4}$$

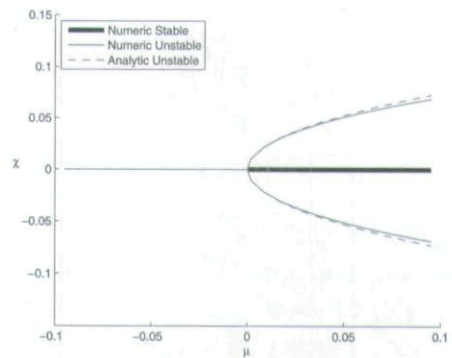
$$N = 4: \quad D_\chi(0, \mu) = 1 - \frac{0.937379\mu}{M}. \tag{7.5}$$

In both (7.4) and (7.5), we see that $\chi^{(n)} = 0$ solutions are stable only for positive values of μ , and can conclude that these pitchfork bifurcations are also subcritical. These results are each compared with a numerical bifurcation analysis in Figs. 4(b) and 4(c). The numerical data in Fig. 4 was plotted to clearly show the similarities and differences in the results predicted by the center manifold for the $N = 2, 3, 4$ cases.

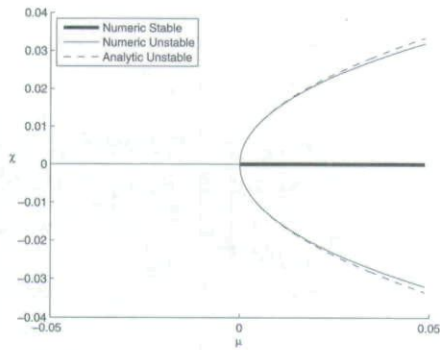
It may seem that the L_b bifurcation points would be subcritical for systems of any number of agents, and the numerical results of Fig. 5 seem to support this conjecture. However, proving this general result analytically with the augmented center manifold reduction has yet to be solved.



(a) Comparison for $N = 2$



(b) Comparison for $N = 3$



(c) Comparison for $N = 4$

Figure 4: The numerical results for the solution branches are compared with those from the center manifold approximated to third order.

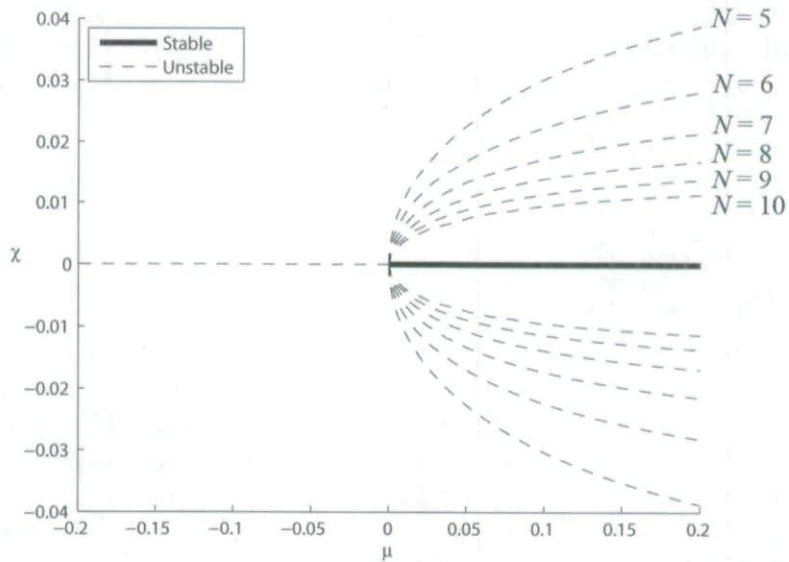


Figure 5: Numerical bifurcation results for $N = 5, \dots, 10$. Here χ refers to the center manifold coordinate for the corresponding N value.

We remark that these results can be applied to the horizontally aligned equilibrium configuration. Here, the vertical equilibrium configuration can be thought of as being rotated by 90° so that the rectangular domain has fixed unit height, while it is the width that is parameterized by L . In this horizontal arrangement, the new aspect ratio can be treated as $1/L$. Therefore, by substituting L by its inverse, similar results can be found for the horizontally aligned equilibrium configuration.

8. Conclusions

In this paper, we considered the stability and bifurcation behavior of the vertically aligned configurations analytically. In particular, we calculated the eigenvalues and eigenvectors associated with the linearization about such equilibrium configurations, identified parameter values at which bifurcations occur, and performed a center manifold reduction for small numbers of agents that captured the asymptotic dynamics of the system near the bifurcation. The analysis of the dynamics reduced to the center manifold allowed us to classify the bifurcation that occurs for the system. In general, we demonstrated that the model is rich with dynamical phenomena that can be used to explain qualitative differences between similar systems, such as how territorial equilibria scale with the size of the domain and the number of agents.

Although we have analyzed a specific bifurcation point of the aligned equilibrium configuration, the methods discussed can in principle be applied to any bifurcation point of any equilibrium in general. For instance, these methods can be applied to the study of asymmetric equilibria in convex polygon domains with non-uniform density functions. Analyzing such a system would be straightforward but tedious in practice.

Acknowledgments The authors would like to thank David A.W. Barton for the use of his numerical continuation code for this system. This work was partially supported by the Institute for Collaborative Biotechnologies through Grant DAAD19-03D004 from the U.S. Army Research Office.

Appendix: alternate method for $N=2$ bifurcation analysis

Here we give a more physically intuitive, exact bifurcation analysis for the simple case when $N=2$, for which there are only two distinct equilibrium configurations: the aligned configuration and an offset configuration [10]. This confirms and helps to clarify, for this special case, the results from the center manifold analysis given in the main text.

According to numerical results found in [10], the equilibrium configurations which bifurcate from the aligned equilibrium configuration have $x_2 = -x_1$ and $y_2 = -y_1$. By evaluating (3.7) for this specific two agent case,

$$c_{x,1}^{(n)} = \frac{x_1}{6Ly_1^{(n)}}, \quad c_{y,1}^{(n)} = \frac{L}{4} - \frac{(x_1^{(n)})^2}{6L(y_1^{(n)})^2}, \quad (\text{A.1})$$

and recalling that the agents in equilibrium are located at their centroids such that $c_{x,1}^{(n)} = x_1^{(n)}$ and $c_{y,1}^{(n)} = y_1^{(n)}$, (A.1) can be solved to obtain

$$x_1^{(n)} = \frac{1}{6} \sqrt{3 - \frac{2}{L^2}}, \quad y_1^{(n)} = \frac{1}{6L}. \quad (\text{A.2})$$

Furthermore, from (3.3), $y_{eq,1} = L/4$. Solving the y_1 expression of (A.2) at $y_{eq,1}$ produces $L = \sqrt{2/3}$, which indicates that a bifurcation occurs because $L = \sqrt{2/3}$ is the only parameter value where the aligned and other equilibrium configurations coincide. Instead, if $L = \mu + \sqrt{2/3}$ is substituted into the x_1 expression of (A.2), the solution for x_1 becomes

$$x_1^{(n)} = \frac{1}{6} \sqrt{3 - \frac{2}{(\mu + \sqrt{2/3})^2}}, \quad y_1^{(n)} = \frac{1}{6L}. \quad (\text{A.3})$$

Expanding in μ , we find for small μ that $x_1^{(n)} = \sqrt{\sqrt{6}\mu/12}$. Lastly, the coordinate transformation ϕ gives

$$\chi^{(n)} = \frac{x_1^{(n)} - x_2^{(n)}}{2} = x_1^{(n)} = \sqrt{\frac{\sqrt{6}\mu}{12}}.$$

The bifurcation solution here agrees with that of the solution found by the center manifold reduction. When compared to the numerical results in Fig. 4(a), we find that (A.3) matches the numerical results exactly.

References

- [1] J. CARR, *Applications of Center Manifold Theory*, Springer-Verlag: New York, Heidelberg, Berlin, 1981.
- [2] J. CORTÉS, S. MARTÍNEZ, T. KARATAS, AND F. BULLO, *Coverage Control for Mobile Sensing Networks*, IEEE Trans. Robotics and Automation, 20, 243-255, 2004.
- [3] Q. DU, V. FABER, AND M. GUNZBURGER, *Centroidal Voronoi Tessellations: Applications and Algorithms*, SIAM Review 41, 637-676, 1999.
- [4] J. GUCKENHEIMER AND P. HOLMES, *Nonlinear Oscillations, Dynamical Systems, and Bifurcations of Vector Fields*, Springer-Verlag New York, Inc., New York, 1983.
- [5] A. GUSRIALDI, S. HIRCHE, T. HATANAKA, AND M. FUJITA, *Voronoi Based Coverage Control with Anisotropic Sensors*, Proceedings of the 2008 American Control Conference, 736-741, 2008.
- [6] M. HASEGAWA, AND M. TANEMURA, *On the Pattern of Space Division by Territories*, Ann. Inst. Statist. Math. 28, 509-519, 1976.
- [7] M. HASEGAWA, AND M. TANEMURA, *Spatial Patterns of Territories*, in: Matusita, K. (Ed.) Recent Developments in Statistical Inference and Data Analysis, North-Holland, Amsterdam, pp. 73-78, 1980.
- [8] C. H. HSIEH, Y.-L. CHUANG, Y. HUANG, K. K. LEUNG, A. L. BERTOZZI, AND E. FRAZZOLI, *An Economical Micro-car Testbed for Validation of Cooperative Control Strategies*, in Proc. 2006 American Control Conference, Minneapolis, Minnesota, pp. 1446-1451, 2006.

- [9] M. TANEMURA, AND M. HASEGAWA, *Geometrical Models of Territory. I. Models for Synchronous and Asynchronous Settlement of Territories*, J. Theor. Biol. 82, 477-496, 1980.
- [10] R. VOTEL, D. A. W. BARTON, T. GOTOU, T. HATANAKA, M. FUJITA, AND J. MOEHLIS, *Equilibrium Configurations for a Territorial Model*, SIAM J. of Appl. Dyn. Syst. 8, 1234-1260, 2009.
- [11] E. O. WILSON, *Sociobiology: The New Synthesis*, Harvard Univ. Press, Cambridge, 1975.
- [12] W. YUEH, *Eigenvalues of Several Tridiagonal Matrices*, Applied Mathematics E-Notes 5, 66-74, 2005.

Copyright of Numerical Mathematics: Theory, Methods & Applications is the property of Global Science Press and its content may not be copied or emailed to multiple sites or posted to a listserv without the copyright holder's express written permission. However, users may print, download, or email articles for individual use.